Physics and Imaging in Radiation Oncology 19 (2021) 102–107

Contents lists available at ScienceDirect

Physics and Imaging in Radiation Oncology

journal homepage: www.sciencedirect.com/journal/physics-and-imaging-in-radiation-oncology

Prostate specific membrane antigen positron emission tomography for lesion-directed high-dose-rate brachytherapy dose escalation

Christopher W. Smith [a,b,c,h,1], Ryan Alfano [a,b,c,h,1], Douglas Hoover [b,c,h], Kathleen Surry [b,c,h], David D'Souza [b,g,h], Jonathan Thiessen [b,c], Irina Rachinsky [d], John Butler [b], Jose A. Gomez [e], Mena Gaed [e], Madeleine Moussa [e], Joseph Chin [f,g], Stephen Pautler [f,g], Glenn S. Bauman [c,g,h], Aaron D. Ward [a,b,c,g,h,*]

[a] Baines Imaging Research Laboratory, 790 Commissioners Rd E, London, ON N6A 5W9, Canada
[b] Lawson Health Research Institute, 750 Base Line Rd E, London, ON N6C 2R5, Canada
[c] Western University Department of Medical Biophysics, 1151 Richmond St., London, ON N6A 3K7, Canada
[d] Western University Department of Medical Imaging, 1151 Richmond St., London, ON N6A 3K7, Canada
[e] Western University Department of Pathology and Laboratory Medicine, 1151 Richmond St., London, ON N6A 3K7, Canada
[f] Western University Department of Surgery, 1151 Richmond St., London, ON N6A 3K7, Canada
[g] Western University Department of Oncology, 1151 Richmond St., London, ON N6A 3K7, Canada
[h] London Regional Cancer Program, 790 Commissioners Rd E, London, ON N6A 4L6, Canada

ARTICLE INFO

Keywords:
Prostate cancer
Positron emission tomography
High dose rate brachytherapy
Dominant intraprostatic lesion
Targeted radiation therapy

ABSTRACT

Background and purpose: Prostate specific membrane antigen positron emission tomography imaging (PSMA-PET) has demonstrated potential for intra-prostatic lesion localization. We leveraged our existing database of co-registered PSMA-PET imaging with cross sectional digitized pathology to model dose coverage of histologically-defined prostate cancer when tailoring brachytherapy dose escalation based on PSMA-PET imaging.

Materials and methods: Using a previously-developed automated approach, we created segmentation volumes delineating underlying dominant intraprostatic lesions for ten men with co-registered pathology-imaging datasets. To simulate realistic high-dose-rate brachytherapy (HDR-BT) treatments, we registered the PSMA-PET-defined segmentation volumes and underlying cancer to 3D trans-rectal ultrasound images of HDR-BT cases where 15 Gray (Gy) was delivered. We applied dose/volume optimization to focally target the dominant intraprostatic lesion identified on PSMA-PET. We then compared histopathology dose for all high-grade cancer within whole-gland treatment plans versus PSMA-PET-targeted plans. Histopathology dose was analyzed for all clinically significant cancer with a Gleason score of 7or greater.

Results: The standard whole-gland plans achieved a median [interquartile range] D98 of 15.2 [13.8–16.4] Gy to the histologically-defined cancer, while the targeted plans achieved a significantly higher D98 of 16.5 [15.0–19.0] Gy ($p = 0.007$).

Conclusion: This study is the first to use digital histology to confirm the effectiveness of PSMA-PET HDR-BT dose escalation using automatically generated contours. Based on the findings of this study, PSMA-PET lesion dose escalation can lead to increased dose to the ground truth histologically defined cancer.

* Corresponding author at: Department of Medical Biophysics, 1151 Richmond Street N, London, ON N6A 5C1, Canada.
E-mail addresses: csmit449@uwo.ca (C.W. Smith), ralfano2@uwo.ca (R. Alfano), douglas.hoover@lhsc.on.ca (D. Hoover), kathleen.surry@lhsc.on.ca (K. Surry), david.dsouza@lhsc.on.ca (D. D'Souza), jonathan.thiessen@sjhc.london.on.ca (J. Thiessen), irina.rachinsky@lhsc.on.ca (I. Rachinsky), jbutler@lawsonimaging.ca (J. Butler), jose.gomezlemus@lhsc.on.ca (J.A. Gomez), mgaed@uwo.ca (M. Gaed), madeleine.moussa@lhsc.on.ca (M. Moussa), joseph.chin@lhsc.on.ca (J. Chin), stephen.pautler@sjhc.london.on.ca (S. Pautler), glenn.bauman@lhsc.on.ca (G.S. Bauman), aaron.ward@uwo.ca (A.D. Ward).
[1] Christopher Smith and Ryan Alfano are co-first authors.

https://doi.org/10.1016/j.phro.2021.07.001
Received 9 December 2020; Received in revised form 30 June 2021; Accepted 1 July 2021

1. Introduction

Prostate cancer recurrence most often originates from the largest and/or highest-grade site of disease [1–3]. These site(s) are termed dominant intraprostatic lesions (DILs). To improve patient outcomes and reduce disease recurrence, treatment methods for prostate cancer that target DILs have begun to emerge. One method is focal dose escalation during radiation therapy. Many studies have confirmed the feasibility of radiation therapy to escalate dose to identified DILs [4–6]. Due to their highly focal nature, brachytherapy techniques such as high dose rate brachytherapy (HDR-BT) may be particularly well-suited to escalate doses to DILs while abiding by dose constraints to surrounding organs at risk [4–8].

Previous studies investigating HDR-BT for focal dose targeting have used multiparametric magnetic resonance imaging (mpMRI) to localize the DIL [9–11]. While mpMRI has been confirmed to be a useful tool for locating the site(s) of disease [12], there has been recent evidence that mpMRI is not enable the observer to delineate all of the cancer, and that interobserver variability could be a confounding issue [13]. An alternative imaging method that has shown promise for prostatic DIL localization is prostate specific membrane antigen (PSMA) positron emission tomography (PET) [14]. Recent work has demonstrated that use of a Gallium-labeled PSMA based radiotracer led to improved sensitivity and specificity for lesion detection confirmed by histopathology, compared to alternative imaging techniques [15]. More recently, a prospective trial reported higher specificities and positive predictive values using PSMA-PET for locating tumor foci within the prostate, compared to mpMRI [16]. A promising radiotracer for PSMA-PET imaging of the DIL is (2-(3-{1-carboxy-5-[(6-18F-fluoro-pyridine-3-carbonyl)-amino]-pentyl}-ureido)-pentanedioic acid) or more commonly referred to as [^{18}F] DCFPyL, [17] which has demonstrated higher spatial resolution than previously-developed Gallium based agents and has the advantage of efficient cyclotron-based production [15].

Challenging the use of PSMA PET imaging in the clinic is the lack of established guidelines regarding standardized uptake value (SUV) thresholds for delineating lesions. Previous studies have attempted to define standardized guidelines through voxel- and region-based analyses. However, they are often limited by their reference standards (e.g. targeted biopsy cores [18] and consensus mapping approaches [19,20]). Whole-mount histology registered to the in-vivo imaging volume serves as the gold standard. However, most studies that have attempted to register histology to in-vivo imaging are limited by the uncertainty of their registration error [21]. Previously, a semi-automated registration algorithm was developed by Gibson et al. to map whole-mount transverse prostate histology to in-vivo MRI with a quantified target registration error [13]. Using this technique, we obtained images from patients using a hybrid PET/MRI scanner and analyzed them retrospectively using an optimal threshold and margin expansion algorithm for lesion delineation developed by Alfano et al. [22].

Using registered digital histology as a reference standard, we aim to answer the following question: does targeting PSMA-PET-defined contours increase the dose to all histologically-defined ground truth cancer while meeting dose constraints to nearby critical structures, in comparison to clinically standard whole-gland treatment planning? We hypothesize that targeting dose to PSMA-PET-defined DIL contours will result in a significant increase in dose to all histologically-defined cancer within the prostate, compared to standard-of-care whole-gland treatment plans.

2. Methods and materials

2.1. PSMA-PET/histology patient population

Under an approved Health Sciences Research Ethics Board study, patients were recruited as part of a multimodality, pre-operative prostate cancer imaging study (n = 20). For further details regarding PET/MRI technical acquisition details and patient inclusion/exclusion criteria, please refer to the Supplementary Material A.I.

A pathology assistant trained in prostate cancer morphology annotated (i.e. graded and segmented) all intra-prostatic lesions on all histology sections, under the supervision of a genitourinary pathologist. All histology annotations were given a Gleason score by the observing clinician, and all were confirmed (or corrected as necessary) by the pathologist [23]. For the purpose of this study, only annotations that had a Gleason score of 7or greater were evaluated. Differentiation of prostate cancer by a Gleason score 7 (3 + 4) or greater and Gleason score 6 or less is concordant with the Kasivisvanathan *et al.* definition of clinically significant and clinically insignificant disease [24]. More details of histological examination can be found in the Supplementary Material A.II.

2.2. Histology to PET/MRI registration

All annotations of cancerous tissue from the mid-gland of the prostate were registered to the in-vivo PET/MRI using a registration procedure that was previously developed by Gibson et al. [13]. In total, ten patients were able to be used for this analysis. More information on the registration of histology to PET/MRI can be found in the Supplementary Material A.II.

2.3. Brachytherapy population

Between July 2015 and December 2016, 30 patients received a single-fraction transrectal ultrasound (TRUS)-guided HDR-BT procedure at our institution. A Profocus 2202 ultrasound machine and an 8848 biplanar probe (BK Medical, Boston, MA) operating at 9 MHz were used to capture all TRUS images. Using a custom manual stepper installed with Vitesse 2.5 (Varian Medical Systems, palo Alto, CA) intra-operative software, axial slices of ultrasound images with 5 mm spacing were acquired as part of the HDR-BT planning.

2.4. PET/MRI to TRUS registration

Each PET/MR image and corresponding histology images were deformably mapped to two different HDR-BT plans in the 30-patient dataset by matching prostates that were close in terms of anatomical similarity (size and shape) (see Supplementary Fig. I). Of the 30 HDR-BT patients, 9 cases had prostate anatomy similar to our PET/MRI cohort and were selected as suitable matches. This registration procedure yielded the mapping of PSMA-PET DILs and the corresponding digital histology annotations to the intraprocedural TRUS imaging space, producing a total of 20 treatment plans (ten patients each mapped to two different treatment plans, where each plan is a unique combination of catheter insertions and dose distributions). PSMA-PET DILs from different patients may be mapped to the same HDR-BT patient in order to meet size and shape constraints for the matching. Further details of the registration are explained in Supplementary Material A.II.

2.5. Standard brachytherapy planning

Standard clinical HDR-BT treatment plans were designed using BrachyVision 13.6 planning software (Varian Medical Systems, Palo Alto, CA) with the intent to deliver the prescription dose to the entire gland as equally as possible while abiding by dose constraints to organs as risk. Treatment plan dose constraints were based on the techniques used by Morton et al. [25] and guidelines outlined by the American Brachytherapy Society, as described by Yamada et al. [26]. Details of the treatment planning dose constraints and objectives are described in Table 1. All standard treatment plans were created using the volume optimization application that is built into BrachyVision.

Table 1
Dose constraints followed during the standard and PSMA targeted HDR-BT treatment planning. (Vxx% is the volume percentage of the structure that received xx% dose of the prescription dose, Dxx% is the prescription dose percentage that xx% of the structure received, Dxxcc is the maximum prescription dose percentage permitted to xx cubic centimeters of volume in that structure).

Organ	Dose Metric	Standard Planning Goal [%]	PSMA-Targeted Planning Goal [%]
Prostate	$V_{90\%}$	≥95	≥95
Prostate	$V_{100\%}$	≥90	≥90
Prostate	$V_{150\%}$	≤35	≤38
Prostate	$V_{200\%}$	≤11	≤14
Urethra	$D_{10\%}$	≤118	≤120
Rectum	$D_{0.5cc}$	≤80	≤80
PSMA-DIL	$D_{98\%}$	N/A	135

2.6. Focal targeting treatment planning

All HDR-BT PSMA-PET targeted treatment plans were designed using BrachyVision 13.6. Each plan was generated by using the volume optimization application that is directly built into BrachyVision. Since these plans were designed with the goal to deliver a focally targeted dose to the PSMA-PET lesion, an adjusted set of dose constraints and dose goals were used and are listed in Table 1. The target dose was 20.3 Gray (Gy) to 98% of the PSMA-PET segmentation which was generated using a threshold of 81% of the maximum SUV, along with a margin expansion of 5.2 mm. More information on the performance of the DIL segmentation on PSMA-PET can be found in the Supplementary Material A.III.

2.7. Dose analysis

To determine if there was any effect of targeted focal dose escalation using PSMA-PET, we calculated the dose the annotated digital histology cancer would have received within the standard HDR-BT treatment plans, and the dose to the corresponding PSMA-PET targeted treatment plans. Specifically, we calculated the minimum dose being delivered to 98% and 90% of the cancer, as well as the mean dose that would have been delivered to each histology annotation.

2.8. Statistics

Prism 5.04 (GraphPad Software, San Diego, CA) was used to perform all statistical analysis. A threshold of $p < 0.05$ was used to deem results significant. Data sets were all subjected to the Shapiro-Wilk test to determine distribution normality. If the data sets were deemed to be normally distributed, a paired *t*-test was used to compare means, while if one of the data sets that were being compared was not normally distributed, the medians were compared using a Wilcoxon matched-pairs signed rank test.

3. Results

The histologically-defined cancer would have received a significantly higher D98 within PSMA-PET targeted treatment plans in comparison to the plans optimized for standard whole-gland treatment, with a median [IQR] D98 of 16.5 [15.0–19.0] Gy compared to 15.2 [13.8–16.4] Gy in the standard plans ($p = 0.007$, Fig. 1). The median D90 to the histologic cancer within the PSMA-PET targeted treatment plans was 19.0 [16.5–21.0] Gy compared to 16.4 [15.0–17.4] Gy for the standard plans ($p = 0.003$, Fig. 1).

In terms of mean dose, the histologically-defined cancer received a significantly higher dose using the PSMA-PET targeted treatment plans. The PSMA-PET targeted plans would have delivered a median [IQR] mean dose of 25.6 [23.7–32.9] Gy, and the standard plans delivered a median mean dose of 21.4 [20.2–22.6] Gy ($p < 0.001$). The percentage of focally-targeted plans that delivered a given D98 dose to the histology is presented in Fig. 2. For example, Fig. 2 demonstrated that the percentage of plans that delivered a D98 of 20 Gy was 0% for standard plans and 20% for PET-targeted plans. Additionally, it was found the

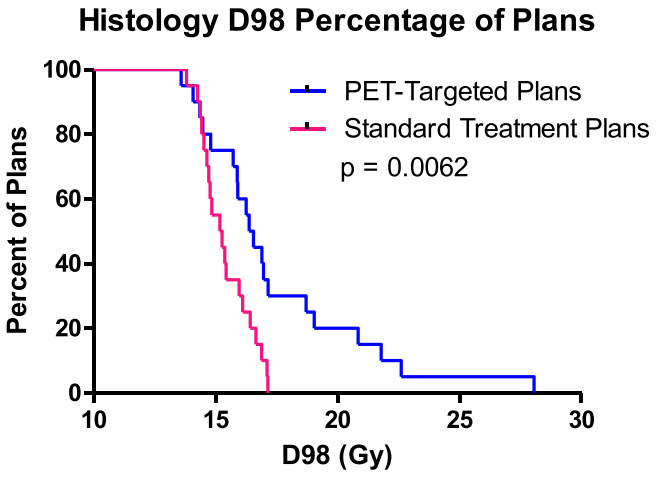

Fig. 2. A line graph displaying the percentage of treatment plans that delivered a given D98 to the histologic cancer. PET-targeted treatment plans are colored in blue and standard treatment plans are colored in magenta. (For interpretation of the references to colour in this figure legend, the reader is referred to the web version of this article.)

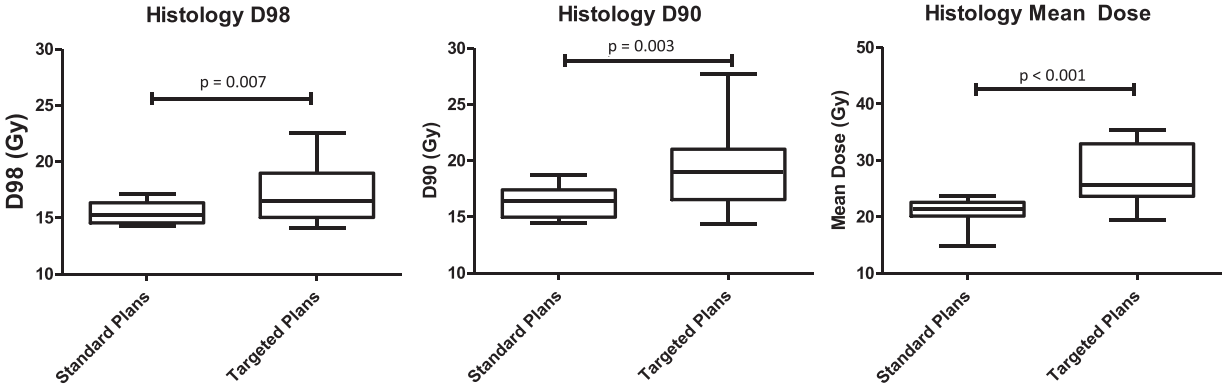

Fig. 1. A box-and-whisker plot of the (left) D98, (middle) D90, and (right) mean doses delivered to the digital histology annotations within PSMA-PET targeted treatment plans and standard treatment plans. The whiskers represent the 10-90th percentiles.

percentage curves were significantly different with a log-rank test ($p = 0.006$). A qualitative result of an ideal boost candidate can be found in Supplementary Fig. II. In terms of dose to the surrounding organs at risk, we did not exceed dose constraints when targeting the DILs. Specifically, we achieved a median prostate V150 of 31.4%, a median prostate V200 of 11.7%, a median urethra D10 of 116.2%, a median rectum D0.5 cc of 62.8%, and a median bladder V80 of 1.2 cm^3.

4. Discussion

We found that by focally escalating the dose to the PSMA-PET segmentations, we were able to achieve a significantly higher D98, D90 and mean dose to the corresponding histologically-defined cancer in comparison to the standard whole-gland designed treatment plans. Additionally, we found that by targeting the PET lesions, we were able to significantly increase the percentage of plans that would have received a higher D98 dose to histologic disease.

In 2016 Gomez *et al.* [9] performed a phase II clinical study that dose-escalated mpMRI DILs using HDR-BT. Using a rigid registration method from mpMRI to TRUS, Gomez successfully escalated dose to targeted lesions to a D98 of 18.7 Gy with acceptable tolerance and toxicity profiles. More recently, Hrinivich *et al.* demonstrated that replanning clinical stereotactic ablative radiotherapy plans by escalating dose towards suspicious PSMA-PET hot spots for oligometastatic prostate cancer resulted in overall increases to the maximum dose to the PTV and decreases to the maximum dose to the OAR [27]. Whereas we used original previously achieved catheter distributions from past treatment plans to target the lesion, additional catheters could be inserted to attempt to further dose escalate the PSMA-PET DILs. In 2019, Wang performed a study that investigated the effect of adding one additional needle on the dose to mpMRI-defined lesions. In that study, they found that mpMRI DILs would receive a V150 of 46.4 ± 28.6% through standard whole-gland planning, while DIL-targeting treatment with the original catheters would achieve a mpMRI V150 of 87.0 ± 15.5%, and targeted plans with an additional targeted needle added would achieve a V150 of 93.0 ± 14.1%. The work performed by Wang demonstrated that the majority of targeted dose can be achieved with the original catheters and that the additional catheter only caused a six percent V150 increase to the mpMRI-defined DIL [10].

These papers have all demonstrated the feasibility of lesion dose escalation, and the localization capabilities of PSMA-PET. Our study adds to these results by not only demonstrating the feasibility of PSMA-PET lesion-directed focal dose escalation, but also confirming the effectiveness of doing so by calculating the dose that would have been delivered to the ground truth histologically-defined cancer. Our PSMA-PET lesions were created using a thresholding guideline of 81% SUV_{max} and a 5.2 mm margin without any user interpretation, and histologic clinically significant cancer was defined in concordance with Kasivivanthan *et al. 2018*, as all cancer with a Gleason score of 7 (3 + 4) or greater [24]. Furthermore, we were able to escalate dose to these targets while maintaining dose constraints to organs at risk. Our constraints were 38% for the prostate V150, 14% for the prostate V200, 120% for the urethra D10, 80% for the rectum D0.5 cc, and while an explicit dose constraint was not used for the bladder, we achieved a nearly identical median V80 to that reported by Morton et al. [25], in which they concluded there was no relationship between bladder dose and genito-urinary toxicity.

Since patients undergo salvage prostatectomy after HDR BT very infrequently, it is rare to obtain post-prostatectomy histology from HDR BT patients. In the rare cases where salvage prostatectomy is done after HDR BT, a substantial amount of time lapses between HDR BT and prostatectomy. Therefore, it is impractical to obtain a PSMA PET/MRI scan, perform HDR BT, perform prostatectomy, and obtain prostatectomy histology all on the same patient, with a short time frame between the PET/MRI scan and obtaining histology. This short time frame is important since the histology must serve as a ground truth for the PSMA PET signal. Therefore, to conduct this study with actual HDR BT catheter implants that capture real spatial inaccuracies and catheter deflections that occur in the clinical setting, we registered prostates on PET/MRI scans taken shortly before surgery from a prostatectomy cohort, to prostates on TRUS containing real HDR-BT catheter implants in a brachytherapy cohort. This approach allowed for testing of PSMA-PET-based lesion targeting on realistic HDR BT catheter distributions with validation against whole-mount prostatectomy histology, which has not been previously reported in the literature.

Several other PET DIL contouring methods have been reported in the literature. Spohn et al. reported on a study aiming to segment the DIL with the [18F]PSMA-1007 PET probe using semi-automatic methods and comparing it to manual user delineation [28]. The authors found that a threshold of 20% of SUVmax achieved a median sensitivity and specificity of 93% and 96%, respectively. The approach the study took is concordant with the approach taken by Alfano et al. with two major differences. First, the registration protocol is based on a manual alignment of in-vivo pre-treatment CT and multi-parametric MRI, which may induce some inherent registration error in mapping histology to PET. The study reported by Alfano et al. used co-registration of histology to in-vivo PET/MRI, eliminating the intermediate manual registration component. Second, the authors in this paper interrogated the more recently-developed [18F]PSMA-1007 radiotracer, compared to [18F]DCF-PyL radiotracer investigated in Alfano et al. [18F]PSMA-1007 has many advantages, including higher signal-to-noise ratio and a lack of urinary excretion of the tracer, meaning that there is no buildup in the bladder. This was one of the limitations of the [18F]DCF-PyL radiotracer used in this study; signal from the bladder may leak into the prostate and may confound uptake in tumor and/or healthy tissue close to the base. Thus, we hypothesize that a focal boosting study against PET-DILs defined from PSMA-1007 would allow for more accurate segmentations to be generated, potentially further improving dose delivery to underlying disease. Fassbender et al. examined a gastrin-releasing peptide receptor-based radiotracer (GRPR) in comparison to a PSMA based radiotracer validated on co-registered histology [29]. This is different than the study performed by Alfano et al. and our study which was only concerned with examining the expression of radio labeled PSMA. Overall, the study indicates that certain tumors have greater expression of GRPR compared to PSMA and vice-versa. Thus, primary prostate cancer may be able to be more accurately defined if information regarding the expression of GRPR and PSMA was provided at the time of imaging. This may be a precursor step in creating DIL contours for focal dose escalation by informing physicians on the type of radiotracer that should be administered and may provide added benefit in terms of increased dose to underlying disease as a result.

The results presented in this paper need to be interpreted in context of the limitations of our study. First, the TRUS and MRI/PET registration error was not evaluated. Previous studies have published the error between TRUS and MRI to between 2.1 mm and 3.5 mm [30,31] for intra-patient registration. However, we performed inter-patient registration to simulate realistic spatial distribution of HDR-BT catheters surrounding the PSMA-PET defined DILs. The critical registration error of our work was the error between the histology and MRI, which was meticulously measured and reported by our group [13] to be less than 2 mm. Also due to our MRI-histology registration algorithm's optimization for registration of transverse, mid-gland histology sections, our data set excluded patients having a DIL in sagittally-sectioned apex and base regions. Second, lesions in the prostate located near the base may be confounded by the high tracer uptake in the bladder. Newer PET imaging agents, such as [^{18}F]PSMA-1007, are not excreted through the urine and might mitigate this interference [32]. Third, our experimentation was also limited to one segmentation algorithm designed to encompass little to no healthy tissue while maximizing the amount of cancerous tissue; future work in this area may revolve around optimizing the thresholding and margin expansion criteria to create contours that cover more histologic disease and achieve higher targeted

doses while maintaining low dose to organs at risk. Fourth, this study was a single-institution retrospective analysis on a small cohort of men with lesions predominantly distal to the urethra; our findings need to be further validated on a larger, multi-institutional data cohort to account for patient and catheter implant variability.

In conclusion, this study is the first to confirm the potential effectiveness of computer generated PSMA-PET lesion directed focal dose escalation using HDR-BT for prostate cancer through the utilization of co-registered digital histology. Our findings suggest that focally escalating dose to PSMA-PET defined mid-gland lesions will lead to significantly higher dose to histologically defined disease.

Data sharing statement

Restricted Access (legal/ethical) on grounds that we do not have patient consent to share their data outside of our hospital setting.

Funding

Funding for this project was provided by:
Natural Sciences and Engineering Research Council of Canada
Prostate Cancer Canada
Canadian Institutes of Health Research
Ontario Institute for Cancer Research

Declaration of Competing Interest

The authors declare that they have no known competing financial interests or personal relationships that could have appeared to influence the work reported in this paper.

Appendix A. Supplementary data

Supplementary data to this article can be found online at https://doi.org/10.1016/j.phro.2021.07.001.

References

[1] Arrayeh E, Westphalen AC, Kurhanewicz J, Roach M, Jung AJ, Carroll PR, et al. Does local recurrence of prostate cancer after radiation therapy occur at the site of primary tumor? Results of a longitudinal MRI and MRSI study. Int J Radiat Oncol Biol Phys 2012;82(5):e787–93. https://doi.org/10.1016/j.ijrobp.2011.11.030.
[2] Cellini N, Morganti AG, Mattiucci GC, Valentini V, Leone M, Luzi S, et al. Analysis of intraprostatic failures in patients treated with hormonal therapy and radiotherapy: implications for conformal therapy planning. Int J Radiat Oncol Biol Phys 2002;53(3):595–9. https://doi.org/10.1016/S0360-3016(02)02795-5.
[3] Pucar D, Hricak H, Shukla-Dave A, Kuroiwa K, Drobnjak M, Eastham J, et al. Clinically significant prostate cancer local recurrence after radiation therapy occurs at the site of primary tumor: magnetic resonance imaging and step-section pathology evidence. Int J Radiat Oncol Biol Phys 2007;69(1):62–9. https://doi.org/10.1016/j.ijrobp.2007.03.065.
[4] Andrzejewski P, Kuess P, Knäusl B, Pinker K, Georg P, Knoth J, et al. Feasibility of dominant intraprostatic lesion boosting using advanced photon-, proton- or brachytherapy. Radiother Oncol 2015;117(3):509–14. https://doi.org/10.1016/j.radonc.2015.07.028.
[5] Crook J, Ots A, Gaztañaga M, Schmid M, Araujo C, Hilts M, et al. Ultrasound-planned high-dose-rate prostate brachytherapy: dose painting to the dominant intraprostatic lesion. Brachytherapy 2014;13(5):433–41. https://doi.org/10.1016/j.brachy.2014.05.006.
[6] Vigneault E, Mbodji K, Racine L-G, Chevrette E, Lavallée M-C, Martin A-G, et al. Image-guided high-dose-rate brachytherapy boost to the dominant intraprostatic lesion using multiparametric magnetic resonance imaging including spectroscopy: results of a prospective study. Brachytherapy 2016;15(6):746–51. https://doi.org/10.1016/j.brachy.2016.09.004.
[7] Thiruthaneeswaran N, Hoskin PJ. High dose rate brachytherapy for prostate cancer: standard of care and future direction. Cancer/Radiother 2016;20(1):66–72. https://doi.org/10.1016/j.canrad.2016.01.001.
[8] Paul R, Hofmann R, Schwarzer JU, Stepan R, Feldmann HJ, Kneschaurek P, et al. Iridium 192 high-dose-rate brachytherapy – a useful alternative therapy for localized prostate cancer? World J Urol 1997;15(4):252–6. https://doi.org/10.1007/BF01367663.
[9] Gomez-Iturriaga A, Casquero F, Urresola A, Ezquerro A, Lopez JI, Espinosa JM, et al. Dose escalation to dominant intraprostatic lesions with MRI-transrectal ultrasound fusion high-dose-rate prostate brachytherapy: prospective phase II trial. Radiother Oncol 2016;119(1):91–6. https://doi.org/10.1016/j.radonc.2016.02.004.
[10] Wang T, Press RH, Giles M, Jani AB, Rossi P, Lei Y, et al. Multiparametric MRI-guided dose boost to dominant intraprostatic lesions in CT-based high-dose-rate prostate brachytherapy. Br J Radiol 2019;92(1097):20190089. https://doi.org/10.1259/bjr.20190089.
[11] Smith CW, Hoover D, Surry K, D'Souza D, Cool DW, Kassam Z, et al. A multiobserver study investigating the effectiveness of prostatic multiparametric magnetic resonance imaging to dose escalate corresponding histologic lesions using high-dose-rate brachytherapy. Brachytherapy 2021;20(3):601–10. https://doi.org/10.1016/j.brachy.2021.01.005.
[12] Shukla-Dave A, Hricak H. Role of MRI in prostate cancer detection. NMR Biomed. 2014;27:16–24. https://doi.org/10.1002/nbm.2934.
[13] Gibson E, Bauman GS, Romagnoli C, Cool DW, Bastian-Jordan M, Kassam Z, et al. Toward prostate cancer contouring guidelines on magnetic resonance imaging: dominant lesion gross and clinical target volume coverage via accurate histology fusion. Int J Radiat Oncol Biol Phys 2016;96(1):188–96. https://doi.org/10.1016/j.ijrobp.2016.04.018.
[14] Maurer T, Eiber M, Schwaiger M, Gschwend JE. Current use of PSMA-PET in prostate cancer management. Nat Rev Urol 2016;13(4):226–35. https://doi.org/10.1038/nrurol.2016.26.
[15] Bauman G, Martin P, Thiessen JD, Taylor R, Moussa M, Gaed M, et al. [(18)F]-DCFPyL positron emission tomography/magnetic resonance imaging for localization of dominant intraprostatic foci: first experience. Eur Urol Focus 2018;4(5):702–6. https://doi.org/10.1016/j.euf.2016.10.002.
[16] Rhee H, Thomas P, Shepherd B, Gustafson S, Vela I, Russell PJ, et al. Prostate specific membrane antigen positron emission tomography may improve the diagnostic accuracy of multiparametric magnetic resonance imaging in localized prostate cancer. J Urol 2016;196(4):1261–7. https://doi.org/10.1016/j.juro.2016.02.3000.
[17] Bouvet V, Wuest M, Jans H-S, Janzen N, Genady AR, Valliant JF, et al. Automated synthesis of [18F]DCFPyL via direct radiofluorination and validation in preclinical prostate cancer models. Eur J Nucl Med Mol Imaging Res 2016;6(1). https://doi.org/10.1186/s13550-016-0195-6.
[18] Lopci E, Saita A, Lazzeri M, Lughezzani G, Colombo P, Buffi NM, et al. 68Ga-PSMA positron emission tomography/computerized tomography for primary diagnosis of prostate cancer in men with contraindications to or negative multiparametric magnetic resonance imaging: a prospective observational study. J Urol 2018;200(1):95–103. https://doi.org/10.1016/j.juro.2018.01.079.
[19] Rahbar K, Weckesser M, Huss S, Semjonow A, Breyholz H-J, Schrader AJ, et al. Correlation of intraprostatic tumor extent with 68Ga-PSMA distribution in patients with prostate cancer. J Nucl Med 2016;57(4):563–7. https://doi.org/10.2967/jnumed.115.169243.
[20] Kesch C, Vinsensia M, Radtke JP, Schlemmer HP, Heller M, Ellert E, et al. Intraindividual comparison of 18F-PSMA-1007 PET/CT, multiparametric MRI, and radical prostatectomy specimens in patients with primary prostate cancer: a retrospective, proof-of-concept study. J Nucl Med 2017;58(11):1805–10. https://doi.org/10.2967/jnumed.116.189233.
[21] Zamboglou C, Fassbender TF, Steffan L, Schiller F, Fechter T, Carles M, et al. Validation of different PSMA-PET/CT-based contouring techniques for intraprostatic tumor definition using histopathology as standard of reference. Radiother Oncol 2019;141:208–13. https://doi.org/10.1016/j.radonc.2019.07.002.
[22] Alfano R, Bauman GS, Liu W, Thiessen JD, Rachinsky I, Pavlosky W, et al. Histologic validation of auto-contoured dominant intraprostatic lesions on [18F]DCFPyL PSMA-PET imaging. Radiother Oncol 2020;152:34–41. https://doi.org/10.1016/j.radonc.2020.08.008.
[23] Chen N, Zhou Q. The evolving Gleason grading system. Chin J Cancer Res 2016;28:58–64. https://doi.org/10.3978/j.issn.1000-9604.2016.02.04.
[24] Kasivisvanathan V, Rannikko AS, Borghi M, Panebianco V, Mynderse LA, Vaarala MH, et al. MRI-targeted or standard biopsy for prostate-cancer diagnosis. N Engl J Med 2018;378(19):1767–77. https://doi.org/10.1056/NEJMoa1801993.
[25] Morton GC, Loblaw DA, Sankreacha R, Deabreu A, Zhang L, Mamedov A, et al. Single-fraction high-dose-rate brachytherapy and hypofractionated external beam radiotherapy for men with intermediate-risk prostate cancer: analysis of short- and medium-term toxicity and quality of life. Int J Radiat Oncol Biol Phys 2010;77(3):811–7. https://doi.org/10.1016/j.ijrobp.2009.05.054.
[26] Yamada Y, Rogers L, Demanes DJ, Morton G, Prestidge BR, Pouliot J, et al. American Brachytherapy Society consensus guidelines for high-dose-rate prostate brachytherapy. Brachytherapy 2012;11(1):20–32. https://doi.org/10.1016/j.brachy.2011.09.008.
[27] Hrinivich WT, Phillips R, Da Silva AJ, Radwan N, Gorin MA, Rowe SP, et al. Online prostate-specific membrane antigen and positron emission tomography–guided radiation therapy for oligometastatic prostate cancer. Adv Radiat Oncol 2020;5(2):260–8. https://doi.org/10.1016/j.adro.2019.10.006.
[28] Spohn SKB, Kramer M, Kiefer S, Bronsert P, Sigle A, Schultze-Seemann W, et al. Comparison of manual and semi-automatic [18F]PSMA-1007 PET based contouring techniques for intraprostatic tumor delineation in patients with primary prostate cancer and validation with histopathology as standard of reference. Front Oncol 2020;10. https://doi.org/10.3389/fonc.2020.60069010.3389/fonc.2020.600690.s001.
[29] Fassbender TF, Schiller F, Zamboglou C, Drendel V, Kiefer S, Jilg CA, et al. Voxel-based comparison of [68Ga]Ga-RM2-PET/CT and [68Ga]Ga-PSMA-11-PET/CT with histopathology for diagnosis of primary prostate cancer. Eur J Nucl Med Mol Imaging Res 2020;10(1). https://doi.org/10.1186/s13550-020-00652-y.

[30] Mayer A, Zholkover A, Portnoy O, Raviv G, Konen E, Symon Z. Deformable registration of trans-rectal ultrasound (TRUS) and magnetic resonance imaging (MRI) for focal prostate brachytherapy. Int J Comput Assist Radiol Surg 2016;11 (6):1015–23. https://doi.org/10.1007/s11548-016-1380-9.

[31] Poulin E, Boudam K, Pinter C, Kadoury S, Lasso A, Fichtinger G, et al. Validation of MRI to TRUS registration for high-dose-rate prostate brachytherapy. Brachytherapy 2018;17(2):283–90. https://doi.org/10.1016/j.brachy.2017.11.018.

[32] Giesel FL, Hadaschik B, Cardinale J, Radtke J, Vinsensia M, Lehnert W, et al. F-18 labelled PSMA-1007: biodistribution, radiation dosimetry and histopathological validation of tumor lesions in prostate cancer patients. Eur J Nucl Med Mol Imaging Res 2017;44(4):678–88. https://doi.org/10.1007/s00259-016-3573-4.